applied sciences

MDPI

Article

Simulation and Fabrication of HfO_2 Thin Films Passivating Si from a Numerical Computer and Remote Plasma ALD

Xiao-Ying Zhang [1], Chia-Hsun Hsu [2], Yun-Shao Cho [2], Shui-Yang Lien [2,*], Wen-Zhang Zhu [1], Song-Yan Chen [3], Wei Huang [3], Lin-Gui Xie [1], Lian-Dong Chen [1], Xu-Yang Zou [1] and Si-Xin Huang [1]

1 School of Opto-electronic and Communication Engineering, Fujian Provincial Key Laboratory of Optoelectronic Technology and Devices, Xiamen University of Technology, Xiamen 361024, China; xyzhang@xmut.edu.cn (X.-Y.Z.); wzzhu@xmut.edu.cn (W.-Z.Z.); x0317621@dyu.edu.tw (L.-G.X.); x0317619@dyu.edu.tw (L.-D.C.); x0317617@dyu.edu.tw (X.-Y.Z.); x0317608@dyu.edu.tw (S.-X.H.)

2 Department of Materials Science and Engineering, Da-Yeh University, ChungHua 51591, Taiwan; cstcaptive@gmail.com (C.-H.H.); yunshaojhuo@gmail.com (Y.-S.C.)

3 Department of Physics, OSED, Xiamen University, Xiamen 361005, China; sychen@xmu.edu.cn (S.-Y.C.); weihuang@xmu.edu.cn (W.H.)

* Correspondence: syl@mail.dyu.edu.tw; Tel.: +886-4-8511888 (ext. 1760)

Received: 31 October 2017; Accepted: 27 November 2017; Published: 1 December 2017

Abstract: Recombination of charge carriers at silicon surfaces is one of the biggest loss mechanisms in crystalline silicon (c-Si) solar cells. Hafnium oxide (HfO_2) has attracted much attention as a passivation layer for n-type c-Si because of its positive fixed charges and thermal stability. In this study, HfO_2 films are deposited on n-type c-Si using remote plasma atomic layer deposition (RP-ALD). Post-annealing is performed using a rapid thermal processing system at different temperatures in nitrogen ambient for 10 min. The effects of post-annealing temperature on the passivation properties of the HfO_2 films on c-Si are investigated. Personal computer one dimension numerical simulation for the passivated emitter and rear contact (PERC) solar cells with the HfO_2 passivation layer is also presented. By means of modeling and numerical computer simulation, the influence of different front surface recombination velocity (SRV) and rear SRV on n-type silicon solar cell performance was investigated. Simulation results show that the n-type PERC solar cell with HfO_2 single layer can have a conversion efficiency of 22.1%. The PERC using silicon nitride/HfO_2 stacked passivation layer can further increase efficiency to 23.02% with an open-circuit voltage of 689 mV.

Keywords: hafnium oxide; atomic layer deposition; crystalline silicon solar cell; annealing

1. Introduction

Reduction of surface recombination is very important for crystalline silicon (c-Si)-based electronic devices, and especially for high-efficiency c-Si solar cells. Because of the increasing need for lower-cost silicon solar cells, as Si material has a rather high cost, thinner Si substrates are required. Conventional surface passivation for Si involves the formation of a thin silicon dioxide (SiO_2) layer. However, this process requires a long period at high temperatures, leading to an increased thermal budget. Due to these process-related issues, low-temperature surface passivation methods for both heavily doped and moderately doped c-Si surfaces have been widely studied. Several materials such as SiC, a-Si:H, and Si_3N_4 have been considered for surface passivation [1]. Recently, Al_2O_3 films grown via atomic layer deposition (ALD) have been reported to have good surface passivation on p-type c-Si [2,3]. ALD provides a very precise control over the properties of the material, especially the uniformity and thickness of dielectric layers. However, an Al_2O_3 passivation layer has negative fixed charges, which result in an inversion layer on the n-type wafer surface, causing short-circuit current loss due to the parasitic shunting between this

inversion layer and metal contact [4]. HfO_2 films have positive fixed charges and this makes it very suitable for passivation of n-type silicon wafers. There is currently limited research focusing on the passivation of HfO_2 on n-type silicon wafers for silicon solar cells [5,6].

In this work, the surface passivation properties of the HfO_2 films deposited by a remote plasma atomic layer deposition system (RP-ALD) on n-type c-Si with different post-annealing temperatures are investigated. The structural changes and the electrical properties of the thin films induced by annealing temperature are characterized. Finally, PC1D (Version 5.9, University of New South Wales, Sydney, NSW, Australia, 2003) simulation for HfO_2-passivated n-type silicon solar cells is presented.

2. Experimental

Double-sided polished (100)-oriented n-type 0.5–1 ohm-cm six-inch 200 µm thick Czochralski Si wafers were cleaned by a standard Radio Corporation of America method, and a 2% hydrogen fluoride-dip for 60 s was performed to remove stray oxides. Approximately 15 nm of HfO_2 (168 cycles) were deposited by remote plasma ALD (Picosun R-200) (Picosun, Espoo, Finland) on the wafers using tetrakis(ethylmethylamino)hafnium (TEMAH) and oxygen as the precursors. The pulse times for TEMAH and O_2 were 1.6 and 10 s, respectively. The nitrogen purge time was 10 s for both precursors. The plasma power was 2500 W. The substrate temperature was 250 °C. The post-deposition rapid thermal anneal was performed in N_2 for 10 min, and the annealing temperature was varied from 400 to 650 °C to investigate the effect on surface passivation. The hydrogenated silicon nitride (SiN_x:H)/HfO_2 stacked layer was prepared and annealed at 500 °C. The SiN_x:H layer with a thickness of 120 nm was deposited using radio-frequency inductively coupled plasma chemical vapor deposition with a gas mixture of trimethylsilane (TMS) and ammonia (NH_3) at a temperature of 120 °C, a power of 1200 W, and a pressure of 5 mTorr. The flow rates of the TMS and NH_3 were 35 and 25 sccm, respectively. The injection level-dependent minority carrier lifetime of the wafers was measured using quasi-steady-state photoconductance (Sinton Instruments WCT-120) (*Sinton Instruments*, Sinton, CO, USA). Assuming an infinite bulk lifetime, a maximum surface recombination rate S_{max} was calculated from the lifetime measurements as given by

$$S_{max} = \frac{W}{2\tau_{eff}} \tag{1}$$

where W is the wafer thickness and τ_{eff} is the measured effective lifetime at an injection level of 1×10^{15} cm^{-3}. For the capacitance–voltage (C–V) measurement, the MOS capacitors with an area of 2×10^{-3} cm^2 were defined by evaporating of Au electrodes onto HfO_2 in high vacuum (1×10^{-6} Torr). The positive oxide charge density (Q_f) was extracted from the C-V curves as given by

$$Q_f = \frac{(\varphi_{ms} - V_{FB})C_{ox}}{qA} \tag{2}$$

where φ_{ms} is the work function difference between the metal and semiconductor, V_{FB} is the flat band voltage, C_{ox} is the oxide capacitance, q is the electron charge, and A is the electrode area. The interface charge density (D_{it}) was calculated from the conductance–voltage curves using the expression [7]

$$D_{it} = \frac{2\omega {C_{ox}}^2 G_{max}}{qA({G_{max}}^2 + \omega^2(C_{ox} - C_m G_{max})^2)} \tag{3}$$

where G_{max} is the maximum conductance, and C_m is the measured capacitance at a frequency ω. The bonding configuration of the HfO_2 films was investigated by Fourier transformation infrared (FTIR) spectroscopy. The cross-sectional images of the HfO_2 films were observed by transmission electron microscopy (TEM). The simulation of solar cell performance was carried out using PC1D computer software.

3. Results and Discussion

Figure 1 shows the FTIR spectra for the HfO_2 films with different post-annealing temperatures ranging from 400 to 650 °C. The absorbance peaks at 415, 512, 600, 623, and 750 cm^{-1} are assigned to Hf–O bonding configuration [8–11]. The peaks at 820, 1000, and 1108 cm^{-1} correspond to the Si–O bonds in the films [8–10]. Considering the as-deposited HfO_2 sample, the Si–O peak at 1108 cm^{-1} suggests that the as-deposited film already consists of an SiO_x-like interfacial layer between the silicon wafer and HfO_2 layer. This is similar to the Al_2O_3/Si system, which attributes the presence of the interfacial SiO_x layer to the first few ALD cycles [12]. The SiO_x peak intensity enhances at the annealing temperature of 400 °C, but it then drops when the annealing temperature further increases. For the annealing temperatures of 550–650 °C, the peak is almost unobservable, which in turn infers that these samples have nearly no SiO_x interfacial layer. On the other hand, the intensity of the Hf–O peak at 623 cm^{-1} increases when the annealing temperature increases. The enhancement of the signal intensity may be a result of densification of the HfO_2 films during the annealing process. It seems that there is a competitive process between the formation of Si–O and Hf–O bonds. Oxygen atoms bond to silicon atoms at low temperatures, but they are consumed by bonding to Hf under high-temperature annealing conditions. Varying the annealing temperature can therefore control the interfacial layer.

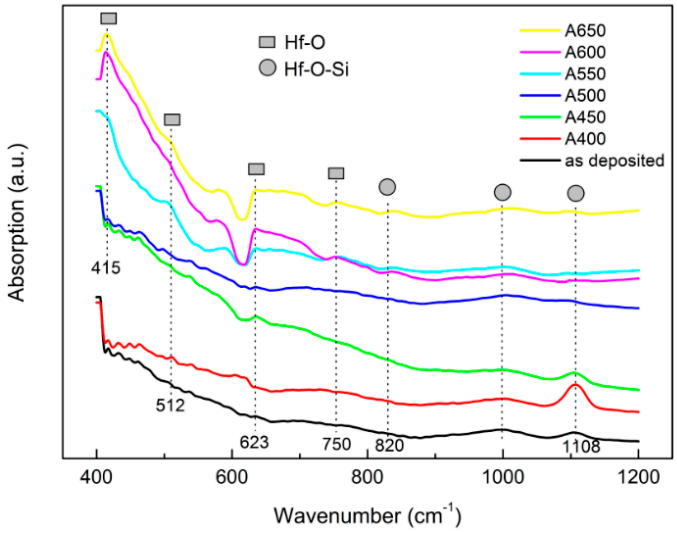

Figure 1. Fourier transformation infrared spectra of HfO_2/Si samples with different annealing temperatures.

Figure 2a shows n-type PERC solar cell structure consisting of an Al_2O_3 emitter passivation layer and an HfO_2 rear passivation layer. The TEM cross-sectional image of the HfO_2/n-type Si interface annealed at 550 °C is shown in Figure 2b. The extent of the atom arrangement order can be used for evaluation of crystallization of films. It can be seen that the atoms in the HfO_2 region are orderly arranged, indicating the high crystallinity achieved at the annealing temperature of 550 °C. The interfacial SiO_x layer with a thickness of approximately 2.5 nm can be seen, but both sides of this interfacial layer are partially crystallized. It has been reported that HfO_2 would be possibly crystallized at temperatures greater than 400 °C [13]. It should be noted that the interfacial layer in the as-deposited sample is approximately 3 nm of amorphous SiO_x .The crystallization near the HfO_2/SiO_2 interface causes a thickness reduction in the actual amorphous SiO_x layer. This phenomenon is more pronounced when the annealing temperature is elevated. In Figure 2b, the amorphous SiO_x layer is significantly inhomogeneous, and the SiO_x layer can hardly be distinguished in some regions. This is in agreement with the decreased signal intensity of SiO_x found via FTIR, as it almost disappears at annealing temperatures greater than 550 °C. As the SiO_x interfacial layer is usually considered to play

an important role in decreasing the interface defect density in the dielectric/Si system [12], annealing temperatures equal to or higher than 550 °C are not preferable.

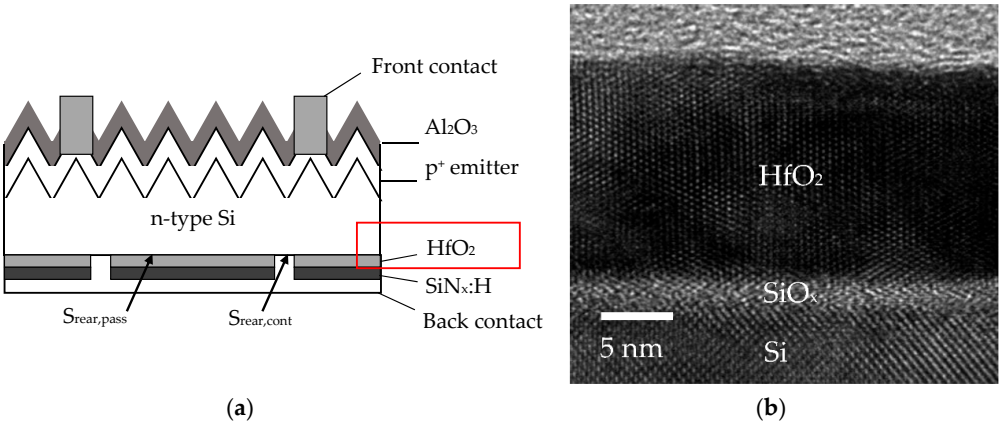

Figure 2. (**a**) n-type passivated emitter and rear contact (PERC) cell structure; (**b**) transmission electron microscopy (TEM) image of the HfO_2/Si interface annealed at 550 °C.

Figure 3 shows the Q_f and D_{it} values obtained from C-V measurements as a function of annealing temperature. The as-deposited film has a high Q_f value of 1.4×10^{13} cm^{-3}. This might be due to the formation of the Si–O interfacial layer, which causes the Hf atoms near the interface region to bond with oxygen atoms in oxygen-poor conditions. The oxygen vacancies are known to be the main cause of positive charges in HfO_2 films [14,15]. The Q_f decreases from 9×10^{12} to 6.9×10^{11} cm^{-2} when the annealing temperature increases from 400 to 650 °C. As shown by the FTIR results, the bonding configuration changes from Si–O to Hf–O, so the oxygen vacancies of HfO_2 near the interface reduce when the annealing temperature increases. Another reason for the smaller Q_f values of the annealed samples compared to the as-deposited one is the crystallization of HfO_2 at these annealing temperatures. In particular, the HfO_2 films are completely crystallized when the annealing temperature reaches 550 °C or above, leading to very low Q_f values of around 0.5×10^{11} cm^{-2}. The value of D_{it} decreases from 5.1×10^{13} $cm^{-2}eV^{-1}$ for the as-deposited sample to a minimum 6.1×10^{12} $cm^{-2}eV^{-1}$ for the sample annealed at 500 °C, and then increases to 1.4×10^{13} $cm^{-2}eV^{-1}$ when the temperature further increases to 650 °C. Several studies have suggested that interfacial SiO_x plays a critical role in the reduction of interface defect density [12]. The high D_{it} of the as-deposited sample is due to the fact that SiO_x deposited at low temperatures has many pores and defects near the SiO_x/Si interface. Increasing the deposition temperature of SiO_x can increase film density, therefore decreasing the D_{it}. However, for the annealing temperatures from 550 and 650 °C, the nearly disappeared SiO_x interfacial layer is responsible for the increased D_{it}.

Table 1 lists the values of τ_{eff} for the HfO_2/Si with different annealing conditions. Lifetimes with two injection levels, 1×10^{14} cm^{-3} ($\tau_{eff,low}$) and 1×10^{15} cm^{-3} ($\tau_{eff,high}$), are specified. The higher injection level corresponds to the evaluation of a solar cell operating under normal conditions, while the degradation of the lifetime at low injection levels can be used for assessing the field effect passivation [16]. In this work, the latter was done by introducing the ratio $\tau_{eff,low}/\tau_{eff,high}$. Note that the passivation of the as-deposited HfO_2/Si sample is poor such that the high-injection-level lifetime is not measurable. The $\tau_{eff,high}$ value increases from 15.2 µs to the maximum of 74.7 µs when the annealing temperature increases from 400 to 500 °C, and it then decreases to 19.4 µs when the temperature further increases to 650 °C. As the 500 °C-annealed sample has the highest lifetime and the lowest D_{it}, this result supports the claim that low D_{it} is the prerequisite of high passivation quality. The ratio of $\tau_{eff,low}$ to $\tau_{eff,high}$ can be divided into two groups. A ratio is around 0.61–0.68 for annealing temperatures of 550–650 °C. This indicates that annealing temperatures equal to or greater than 550 °C can deteriorate the field effect passivation. This is also in agreement with the low Q_f values of these

samples. On the other hand, annealing temperatures of 400, 450, and 500 °C result in a ratio around 0.9–0.94. The high values and small variation indicate that the Q_f of 4.4 × 10^{12} cm^{-3} is enough to achieve field-effect passivation.

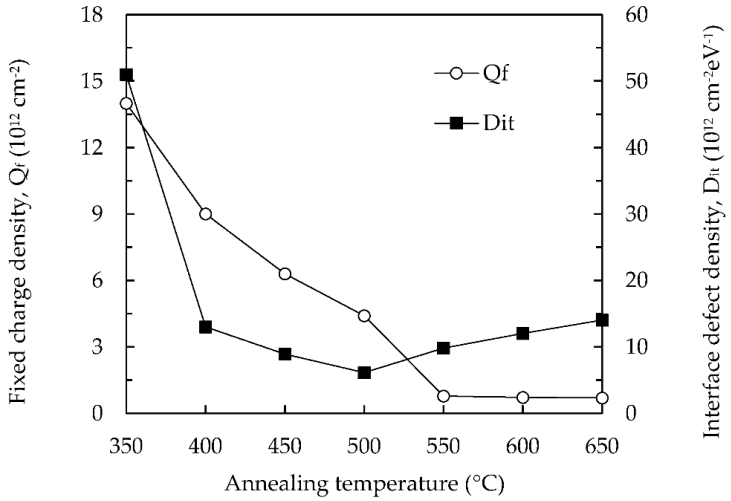

Figure 3. Fixed charge density (Q_f) and interface defect density (D_{it}) of the HfO_2-passivated Si wafers with different annealing temperatures.

Table 1. Low- and high-injection-level minority carrier lifetime and their ratios for the HfO_2-passivated silicon wafers at different annealing temperatures.

Temperature (°C)	$\tau_{eff,low}$ (μs)	$\tau_{eff,high}$ (μs)	$\tau_{eff,low}/\tau_{eff,high}$
As-deposited	0.5	-	-
400	14.3	15.2	0.94
450	44.8	48.2	0.93
500	67.2	74.7	0.9
550	18.5	27.3	0.68
600	14.3	22.1	0.65
650	11.8	19.4	0.61

In order to obtain the influence of the annealing temperature on the performance of n-type PERC solar cells, PC1D simulation was performed. The detailed simulation parameters are summarized in Table 2, and the cell structure is shown in Figure 2a. Some values are taken from the literature [17]. The most important thing to assess the performance of PERC solar cells is the open-circuit voltage (V_{oc}), which can be calculated using the one-diode equation:

$$V_{oc} = \frac{kT}{q} \ln\left(\frac{J_L}{J_{0b} + J_{0e}} + 1\right) \quad (4)$$

where k is the Boltzmann constant, T is the temperature, q is the electron charge, J_L is the generated light current, J_{0b} is the base saturation current density, and J_{0e} is the emitter saturation current. The rear surface passivation affects the value of J_{0b}, which is given by

$$J_{0b} = \frac{qn_i^2 D_p}{LN_D} \frac{S_{rear,eff} \cosh\left(\frac{W}{L}\right) + \frac{D_p}{L} sinh\left(\frac{W}{L}\right)}{\frac{D_p}{L} \cosh\left(\frac{W}{L}\right) + S_{rear,eff} \sin h\left(\frac{W}{L}\right)} \quad (5)$$

where n_i is the intrinsic concentration of silicon, D_p is the hole diffusion coefficient, L is the diffusion length, and N_D is the n-type silicon doping concentration. It should be noted that, as a PERC solar cell has local openings on the rear side, the silicon wafer is in contact with either the HfO_2 passivation layer

or the back metal contact, so two types of rear recombination can be considered, which are designated by $S_{rear,pass}$ and $S_{rear,cont}$, respectively. Thus, the effective rear recombination rate ($S_{rear,eff}$) can be given as [18]

$$S_{rear,eff} = \frac{D_p}{W}\left(\frac{p}{2W\sqrt{\pi f}}\arctan\left(\frac{2W}{p}\sqrt{\frac{\pi}{f}}\right) - \exp\left(-\frac{W}{p}\right) + \frac{D_p}{fWS_{rear,\,cont}}\right)^{-1} + \frac{S_{rear,\,pass}}{1-f}. \quad (6)$$

The contact pitch (p) is 250 µm, and the back contact fraction (f) is 2%—the same as that of industrial PERC cells. Therefore, we can obtain the corresponding $S_{rear,eff}$ for different annealing conditions.

Table 2. Simulation parameters for n-type passivated emitter and rear contact (PERC) solar cells with an HfO_2 passivation layer.

Parameter	Value
[1] Front surface texture depth	3 µm
[1] Exterior front reflectance	3%
[1] Exterior rear reflectance	100%
[2] Internal rear reflectance	90%
[2] Emitter contact	2.48×10^{-3} ohm
[2] Base contact	1×10^{-6} ohm
[1] Wafer thickness, W	200 µm
[1] n-type background doping, N_D	10^{16} cm^{-3}
[1] P^+ emitter doping	10^{20} cm^{-3}
[1] P^+ emitter diffusion depth	0.4 µm
[1] Bulk lifetime, L	1000 µs
[2] Emitter saturation current density, J_{0e}	50 fA/cm^2
[1] Effective rear surface recombination, $S_{rear,eff}$	variable

[1] Obtained by measurement; [2] Obtained in reference [17].

Figure 4 shows the performance in terms of such parameters as V_{oc}, short-circuit current density (J_{sc}), fill factor (FF), and conversion efficiency (η) of the n-type PERC solar cells with different HfO_2 annealing temperatures. It should be noted that here we only consider the single HfO_2 passivation layer, instead of the SiN_x:H/HfO_2 stacked passivation layer. In Figure 4a, V_{oc} varies from 651 mV to its maximum 672.2 mV when the annealing temperature increases from 400 to 500 °C, and then drops to 653.8 mV when the annealing temperature is further increased. J_{sc} and FF show slight variation as compared to V_{oc}. Overall, the conversion efficiency changes ranging between 20.8% and 22.1%, and the trend is similar to that of V_{oc}, as it is the most sensitive parameter when the rear surface recombination rate changes.

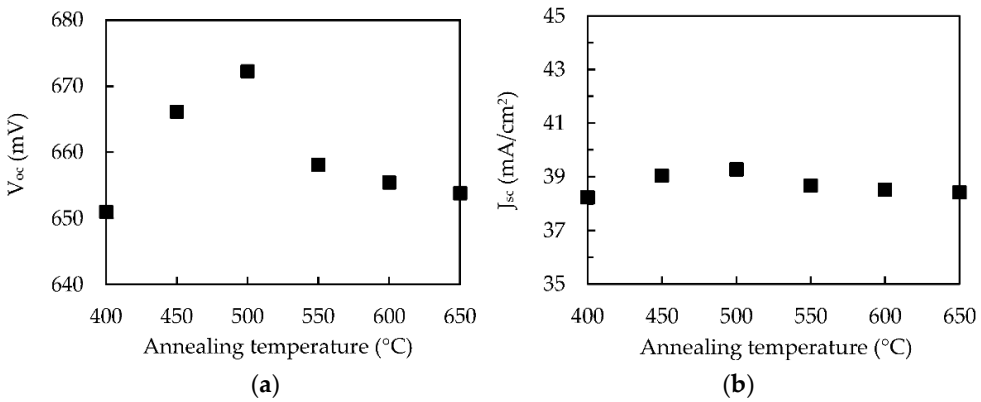

Figure 4. *Cont.*

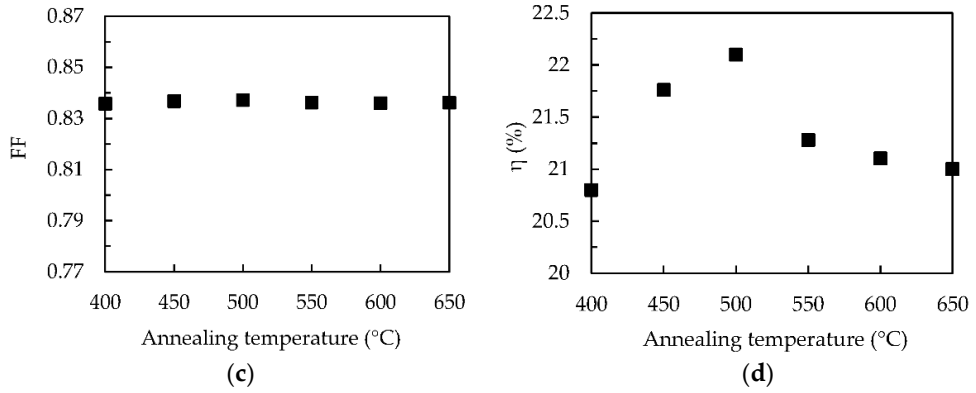

Figure 4. Photovoltaic performance, in terms of (**a**) open-circuit voltage (V_{oc}), (**b**) short-circuit current density (J_{sc}), (**c**) fill factor (FF), and (**d**) conversion efficiency (η), of the n-type PERC solar cells as a function of anneling temperature.

Figure 5 shows simulated V_{oc} and η as a function of base saturation current density. In this work, J_{ob} values of 180–460 fA/cm^2 are obtained for the single HfO_2 rear passivation layer. For PERC solar cells with an SiN_x:H/HfO_2 layer, we obtain a $S_{rear,eff}$ of 22 cm/s with a J_{0b} of 64 fA/cm^2, a V_{oc} of 689 mV, and an η of 23.02%. This great improvement might be because the SiN_x:H layer can provide hydrogen atoms diffusing toward the substrate surface to further passivate the SiO_x/Si interface, similar to the case of the SiN_x:H/Al_2O_3 structure [19,20]. From Equation (5), the lower limit of J_{0b} is 33.9 fA/cm^2, corresponding to V_{oc} of 694 mV and an η of 23.28% for the ideal rear passivation ($S_{rear,pass}$ = 0). The small gap between the cell with ideal passivation and the cell with an SiN_x:H/HfO_2 stacked layer indicates the high passivation quality of the HfO_2-based technique for n-type PERC solar cells.

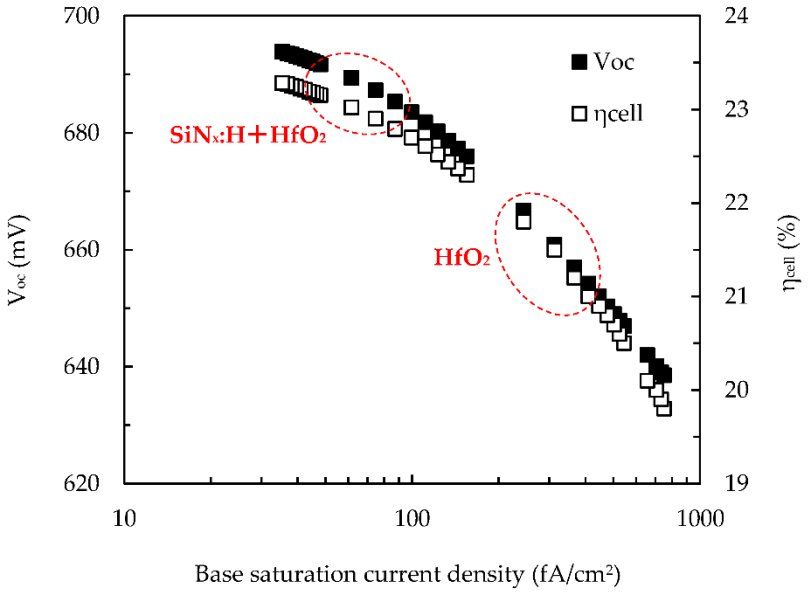

Figure 5. Open-circuit voltage and conversion efficiency of n-type PERC solar cells as a function of base saturation current density.

4. Conclusions

In this study, the HfO_2 thin films were deposited using a remote plasma ALD system on n-type silicon wafers. At the annealing temperature greater than 500 °C, the FTIR spectra show that the SiO_x peak disappears, and this is responsible for the decrease in minority carrier lifetime of silicon

wafers. The annealing temperature of 500 °C was the highest, with the lowest D_{it} and intermediate Q_f. The PC1D simulation result shows that the n-type PERC cell with an HfO_2 single layer can have a conversion efficiency of 22.1%, while the SiN_x:H/HfO_2 stacked passivation layer with a surface recombination rate down to 22 cm/s can improve the conversion efficiency to as high as 23.02% with a V_{oc} of 689 mV. The small gap between the cell with ideal passivation and the cell with the SiN_x:H/HfO_2 stacked layer indicates great passivation quality of the HfO_2-based technique for n-type PERC solar cells.

Acknowledgments: This work is sponsored by the Ministry of Science and Technology of the Republic of China under the grants Nos. 105-2632-E-212-001 and 104-2221-E-212-002-MY3.

Author Contributions: Xiao-Ying Zhang, Shui-Yang Lien, and Chia-Hsun Hsu designed and performed the experiment. Xiao-Ying Zhang and Chia-Hsun Hsu wrote the manuscript. Yun-Shao Cho, Wen-Zhang Zhu, Song-Yan Chen, and Wei Huang assisted in material characterization. Lin-Gui Xie, Lian-Dong Chen, Xu-Yang Zou, and Si-Xin Huang contributed to the valuable discussion on experimental and theoretical results, respectively. All authors read and approved the final manuscript.

Conflicts of Interest: The authors declare no conflict of interest.

References

1. Rahman, M.Z. Advances in surface passivation and emitter optimization techniques of c-Si solar cells. *Renew. Sustain. Energy Rev.* **2014**, *30*, 734–742. [CrossRef]
2. Albadri, A.M. Characterization of Al_2O_3 surface passivation of silicon solar cells. *Thin Solid Films* **2014**, *562*, 451–455. [CrossRef]
3. Simon, D.K.; Jordan, P.M.; Dirnstorfer, I.; Benner, F.; Richter, C.; Mikolajick, T. Symmetrical Al_2O_3-based passivation layers for p- and n-type silicon. *Sol. Energy Mater. Sol. Cells* **2014**, *131*, 72–76. [CrossRef]
4. Dauwe, S.; Mittelstädt, L.; Metz, A.; Hezel, R. Experimental evidence of parasitic shunting in silicon nitride rear surface passivated solar cells. *Prog. Photovolt. Res. Appl.* **2002**, *10*, 271–278. [CrossRef]
5. Cui, J.; Wan, Y.; Cui, Y.; Chen, Y.; Verlinden, P.; Cuevas, A. Highly effective electronic passivation of silicon surfaces by atomic layer deposited hafnium oxide. *Appl. Phys. Lett.* **2017**, *110*, 021602. [CrossRef]
6. Wang, J.; Sadegh Mottaghian, S.; Farrokh Baroughi, M. Passivation properties of atomic-layer-deposited hafnium and aluminum oxides on Si surfaces. *IEEE Trans. Electron Devices* **2012**, *59*, 342–348. [CrossRef]
7. Oulachgar, E.; Aktik, C.; Scarlete, M.; Dostie, S.; Sowerby, R.; Gujrathi, S. Electrical and optical characterization of SiONC dielectric thin film deposited by polymer-source chemical vapor deposition. *J. Appl. Phys.* **2007**, *101*, 084107-1–084107-5. [CrossRef]
8. Singh, V.; Sharma, S.K.; Kumar, D.; Nahar, R.K. Study of rapid thermal annealing on ultra thin high-k HfO_2 films properties for nano scaled MOSFET technology. *Microelectron. Eng.* **2012**, *91*, 137–143. [CrossRef]
9. Yan, K.; Yao, W.; Zhao, Y.; Yang, L.; Cao, J.; Zhu, Y. Oxygen vacancy induced structure change and interface reaction in HfO_2 films on native SiO_2/Si substrate. *Appl. Surf. Sci.* **2016**, *390*, 260–265. [CrossRef]
10. Deshpande, A.; Inman, R.; Jursich, G.; Takoudis, C.G. Annealing behavior of atomic layer deposited hafnium oxide on silicon: Changes at the interface. *J. Appl. Phys.* **2006**, *99*, 094102. [CrossRef]
11. Neumayer, D.A.; Cartier, E. Materials characterization of ZrO_2-SiO_2 and HfO_2-SiO_2 binary oxides deposited by chemical solution deposition. *J. Appl. Phys.* **2001**, *90*, 1801–1808. [CrossRef]
12. Hoex, B.; Heil, S.B.S.; Langereis, E.; Van DeBanden, M.C.M.; Kessels, W.M.M. Ultralow surface recombination of c-Si substrates passivated by plasma-assisted atomic layer deposited Al_2O_3. *Appl. Phys. Lett.* **2006**, *89*, 042112. [CrossRef]
13. Srivastava, V.M.; Yadav, K.S.; Singh, G. Double-Pole Four-Throw RF CMOS switch design with double-gate transistors. In Proceedings of the 2010 Annual IEEE India Conference: Green Energy, Computing and Communication, INDICON 2010, Kolkata, India, 17–19 December 2010.
14. McIntyre, P. Bulk and Interfacial Oxygen Defects in HfO_2 Gate Dielectric Stacks: A Critical Assessment. *ECS Trans.* **2007**, *11*, 235–249. [CrossRef]
15. Foster, A.S.; Lopez Gejo, F.; Shluger, A.L.; Nieminen, R.M. Vacancy and interstitial defects in hafnia. *Phys. Rev. B Condens. Matter Mater. Phys.* **2002**, *65*, 1741171–17411713. [CrossRef]
16. Ma, F.J.; Hoex, B.; Samudra, G.S.; Aberle, A.G. Modelling and simulation of field-effect surface passivation of crystalline silicon-based solar cells. *Energy Procedia* **2012**, *15*, 155–161. [CrossRef]

17. Huang, H.; Lv, J.; Bao, Y.; Xuan, R.; Sun, S.; Sneck, S.; Li, S.; Modanese, C.; Savin, H.; Wang, A.; et al. 20.8% industrial PERC solar cell: ALD Al_2O_3 rear surface passivation, efficiency loss mechanisms analysis and roadmap to 24%. *Sol. Energy Mater. Sol. Cells* **2017**, *161*, 14–30. [CrossRef]
18. Fischer, B. Loss Analysis of Crystalline Silicon Solar Cells Using Photoconductance and Quantum Efficiency Measurements. Ph.D. Thesis, Konstanz University, Konstanz, Germany, 15 May 2003.
19. Bordihn, S.; Mertens, V.; Engelhart, P.; Kersten, F.; Mandoc, M.M.; Muller, J.W.; Kesselsb, W.M.M. Surface Passivation by Al_2O_3 and a-SiN_x: H Films Deposited on Wet-Chemically Conditioned Si Surfaces. *ECS J. Solid State Sci. Technol.* **2012**, *1*, P320–P325. [CrossRef]
20. Dingemans, G.; Beyer, W.; van deSanden, M.C.M.; Kessels, W.M.M. Hydrogen induced passivation of Si interfaces by Al_2O_3 films and SiO_2/Al_2O_3 stacks. *Appl. Phys. Lett.* **2010**, *97*, 152106-1–152106-3. [CrossRef]